



SPE 75710

Laboratory and Field Observations of an Apparent Sub Capillary-Equilibrium Water Saturation Distribution in a Tight Gas Sand Reservoir

K.E. Newsham, SPE, Anadarko Petroleum Corp., J.A. Rushing, SPE, Anadarko Petroleum Corp., A. Chauouche, Anadarko Petroleum Corp., and D.B. Bennion, SPE, Hycal Energy Research Laboratories, Ltd

Copyright 2002, Society of Petroleum Engineers Inc.

This paper was prepared for presentation at the SPE Gas Technology Symposium held in Calgary, Alberta, Canada, 30 April–2 May 2002.

This paper was selected for presentation by an SPE Program Committee following review of information contained in an abstract submitted by the author(s). Contents of the paper, as presented, have not been reviewed by the Society of Petroleum Engineers and are subject to correction by the author(s). The material, as presented, does not necessarily reflect any position of the Society of Petroleum Engineers, its officers, or members. Papers presented at SPE meetings are subject to publication review by Editorial Committees of the Society of Petroleum Engineers. Electronic reproduction, distribution, or storage of any part of this paper for commercial purposes without the written consent of the Society of Petroleum Engineers is prohibited. Permission to reproduce in print is restricted to an abstract of not more than 300 words; illustrations may not be copied. The abstract must contain conspicuous acknowledgment of where and by whom the paper was presented. Write Librarian, SPE, P.O. Box 833836, Richardson, TX 75083-3836, U.S.A., fax 01-972-952-9435.

Abstract

This paper documents laboratory and field observations of an apparent sub capillary-equilibrium, water saturation distribution in the Bossier tight gas sands. These observations are validated with consistent measurements from several different techniques, including production performance analysis, reservoir fluid phase behavior, log evaluation, and both conventional and special core analyses. We also identify several mechanisms, including those associated with a basin-centered gas system that may be responsible for this phenomenon.

Introduction

Tight gas sands constitute a significant percentage of the U.S. natural gas resource base and offer tremendous potential for future reserve growth and production. A recent study by the Gas Technology Institute¹ indicated tight gas sands comprise almost 70% of gas production from all unconventional gas resources and account for 19% of the total gas production from both conventional and unconventional sources in the U.S. The same study¹ estimated total producible tight gas sand resources exceed 600 tcf, while economically recoverable reserves are 185 tcf. This paper focuses on one of the most active domestic U.S. tight gas sand plays, the Bossier Sands in the East Texas Basin. Specifically, we present results from a reservoir description and characterization study in the Mimms Creek and Dew Fields in Freestone County, Texas.

Similar to conventional oil and gas systems, tight gas sands

are often described by complex geological and petrophysical systems as well as heterogeneities at all scales. Unlike conventional reservoirs, however, tight gas sands often exhibit unique gas storage and producing characteristics. Consequently, effective exploitation of these resources requires accurate description of key reservoir parameters, particularly water saturation. This paper presents results of a Bossier tight gas sand characterization study from which capillary pressure data indicated a very high connate water saturation distribution throughout the entire vertical column. Yet, these low-permeability Bossier sands produce at economically viable rates even though relative permeability measurements suggest these rates are not possible unless the initial water saturation is lower than that predicted by capillary equilibrium. We attribute this anomalous production behavior to the presence of a sub capillary-equilibrium distribution of water saturation, *i.e.*, an unusually low water saturation distribution that cannot be predicted by capillary equilibrium.

We present laboratory and field observations of the Bossier sands, a deep abnormally-pressured, high-temperature tight gas sand reservoir exhibiting an apparent sub capillary-equilibrium water saturation distribution. These observations are based upon consistent measurements obtained from several different techniques, including production performance analysis, reservoir fluid phase behavior, log evaluation, and both conventional and special core analyses. We provide a detailed description of the analysis techniques used in our study and discuss specific results that indicate an unusually low water saturation distribution. We also identify several mechanisms, including those associated with a basin-centered gas system, that may be responsible for the long-term desiccation or evaporation of the initial, immobile, connate water saturation.

Regional Geology and Depositional Environment

The Bossier sands are Upper Jurassic in age and were deposited in the East Texas Basin. Located in northeast Texas, this sedimentary basin is a deep elongated trough structure with shelf-slope systems on the basin flanks. Several major tectonic features, including the Sabine Uplift to the east,

the Mexia-Talco Fault System to the north and west, and the Angelina-Caldwell Flexure to the south² bound the basin. East Texas is recognized as one of three major salt provinces in the U.S.. The East Texas Basin is characterized by major salt features - salt anticlines, piercement domes, pillows, *etc.* - within its interior.² Current geological models suggest a relationship between generation of the major fault systems, salt deformation and migration, basin subsidence, and sediment deposition during middle to late Mesozoic.² The significant salt structures also appear to control the distribution of sediments within the basin interior.²

A typical stratigraphic column for the East Texas Basin (Fig. 1) shows that the Bossier sands are part of the Upper Jurassic Cotton Valley Group and are overlain by the Cotton Valley Sandstone.² The Bossier interval is thick and lithologically complex and contains black to gray-black shale interbedded with very fine to fine-grained argillaceous sandstone. Similarly, the Cotton Valley Sandstones are comprised of interbedded shale, and very quartz rich sandstone layers. The Cotton Valley Group is underlain regionally by the Upper Jurassic Louark Group. This includes other hydrocarbon-bearing formations such as the Smackover carbonates and Haynesville/Cotton Valley Limestones. Overlying the Cotton Valley Group is the regionally productive, Lower Cretaceous Travis Peak and Pettit (Sligo) formations. .

As illustrated by the generalized regional dip-section in Fig. 2, Bossier deposition represents cycles of sand progradation into the basin onto organic rich mud, succeeded by marine transgression. Much of the Bossier interval down-dip appear to be time equivalent to the Cotton Valley Sandstone up-dip and represent pro-delta/delta front material related to Cotton Valley deltaic systems.^{2,3} The Bossier sands appear to originate from the north and west and are transported downslope by slumping, debris flow, and turbidity currents. Significant Bossier sand thickness are located in topographic lows created by a combination of faulting, subsidence, and salt movement in the basin.

Bossier Sand Characteristics the Mimms Creek and Dew Fields

The current Bossier sand play is centered along the western shelf margin of the East Texas Basin, specifically in Robertson, Leon, Limestone, and Freestone counties. In this section we summarize the reservoir characteristics of the Mimms Creek and Dew Fields in Freestone County. Much of the reservoir description is based on more than 500 ft of whole core and more than 100 rotary sidewall core samples. Most of the whole core was obtained using a low-invasion, oil-base mud system.

Bossier Sand Facies. The Bossier sands in Mimms Creek and Dew Fields are comprised of a series of stacked sandy packages as illustrated by the type log in Fig. 3. In chronological order of deposition, these packages are known as the York, Bonner, Shelley, and Moore sands. Stratigraphic

sequences observed from several whole cores indicate the sands were deposited as a prograding sediment wedge complex during a lowstand onto organic shelf mud deposited during a highstand. At the top of the sand packages, ravinement or transgressive lag deposits have been observed indicating the onset of a marine transgression during which very little sand was preserved above wave base. The Bossier sands are capped by restricted to open shelfal muds deposited during another highstand.³

Typical Bossier sand body geometry is elongated and oriented with the long axis parallel to the depositional dip. (Fig. 4.) Consequently, lateral sand continuity along depositional strike is often limited, resulting in sands with small dimensions and limited continuity. The sand body thickness varies from tens to several hundred feet. The combination of low depositional relief and limited lateral sand continuity minimizes the hydrocarbon column height potential within each sand body. The limited geometry of the isolated sand bodies, the low permeability, and high degree of heterogeneity limits the volume of recoverable gas by a single well. This observation is confirmed from production decline type curve analysis that indicates small drainage areas, typically less than 40 acres per well.

Bossier Shale Characteristics. The Bossier shales are prevalent both areally and vertically in Mimms Creek and Dew Fields. Laterally extensive shales appear to be seals for the sands, while local shales interbedded in the sand also appear to be the hydrocarbon source for the Bossier sands. A reservoir study of these shales shows current total organic carbon (TOC) ranges from 1% to 5%, while the kerogen type is mixed Type II and III. Vitrinite reflectance measurements range from 1.2 to 1.4 indicating the shales are in the gas window for hydrocarbon generation. Measurements using the RockEval⁴ technique validated the observations from the vitrinite reflectance data.

As we will discuss in the next section, most of the Bossier section in the Mimms Creek and Dew Fields is abnormally overpressured. A probable source for this overpressured system is gas generation from the shales. The data suggests hydrocarbons have been generated not only from kerogen cracking in the shales but also from cracking of liquid hydrocarbons trapped in the sands. This process has been documented by Hunt.⁵ The liquid cracking phenomenon has been postulated on the basis of pyrobitumen observed in core thin sections.

We also believe the gas is of thermal origin on the basis of gas isotope analysis. The computed carbon isotope separations ($\delta^{13}\text{C}$) range from -30% ppt to -40 ppt which is consistent with gases of thermal origin. Gases produced from the Mimms Creek and Dew Fields are composed primarily of methane, but we also measure ethane and small quantities of propane which is also indicative of thermal rather than biogenic origin.

Pressure and Temperature Gradients. The Bossier Sands are overpressured throughout most of the East Texas Basin, including in the Mimms Creek and Dew Field area. As illustrated by Fig. 3, pressure gradients range from 0.50 to 0.55 psi/ft in the upper Cotton Valley Sands, 0.60 to 0.65 psi/ft in the upper Bossier Moore and Shelley Sands, and 0.70 to 0.90 psi/ft in the lower Bossier Bonner and York Sands. The Cotton Valley Sand pressure gradient represents a normal to slightly abnormal pressure gradient of a very saline formation water column (>220 kppm NaCl). A pressure transition exists throughout the Bossier interval with the pressure gradient increasing with depth in a basinward direction.

This overpressured system, which has been confirmed using both static bottomhole pressure measurements and from log analysis, is easily recognized by pressure-depth profiles. The deviation from the normal pressure gradient is referred to as the top of abnormal pressure (TAG) point. The overpressure gradient, when calculated from mean sea level, increases with depth; however, the pressure transition trend, referred to as the incremental pressure gradient (IPG), ranges from 3.5 psi/ft to 5.00psi/ft. Note that the IPG is significantly greater than the lithostatic gradient. The inequality between the lithostatic and incremental pressure gradients suggests the source of overpressure is not caused by compaction/disequilibrium^{6,7}. We do believe, however, that the source of overpressure is caused primarily by hydrocarbon generation and secondarily by chemical compaction effects of diagenesis.

Bossier sands in this area and throughout the East Texas Basin also exhibit abnormally high temperature gradients. Bottomhole temperatures in the Mimms Creek and Dew Fields range from 280°F to 325°F at depths ranging from 12,500 ft to 13,500 ft. This corresponds to temperature gradients of 2.2 to 2.4°F per 100 ft of depth.

Bossier Production Characteristics. The average initial gas production rates vary from 2 to 5 MMscfd in the Moore and Shelley sands, while the Bonner and York sands range from 5 to 15 MMscfd. Similarly, the estimated ultimate gas recovery ranges from 1.5 to 3 Bcf in the Moore and Shelley sands and 3 to 10 Bcf in the Bonner and York. Most wells exhibit hyperbolic decline with stabilized rates of 500 to 900 Mscfd after two to three years. The differences between producing characteristics in the sands reflects both better reservoir quality and higher pressures in the Bonner and York sands.

The Bossier sands also produce some water. The initial water production rates, which range from 50 to 100 bbl/d for the first one to three months, can be attributed to clean-up of stimulation fluids. However, most wells produce between 1 to 5 bbl/day for the life of the well. Because of the low permeability of the Bossier sands, we do not believe a mobile liquid phase exists in the reservoir. The source of long-term water production is probably condensed water vapor. This observation seems to be confirmed by the low salinity of the produced waters.

Bossier Fluid Properties. Wells completed in the Bossier sands produce a wet gas with specific gravity ranging from 0.58 to 0.61. Condensate production averages one to three STB/MMscf over the life of the well. Gas composition typically averages 94 mole% methane and 2 mole% ethane. The remaining hydrocarbon mixture includes fractional percentages of propane through hexane with typically no heptanes plus. Non-hydrocarbon components include 2 to 2.5 mole% carbon dioxide, 0.2 to 0.5 mole% nitrogen, and relatively no hydrogen sulfide.

As we discussed previously, the Bossier produces some water; however, we believe that no mobile liquid water phase exists in the reservoir. Laboratory analyses indicate that five to seven mole% of water vapor may be dissolved in the gas at reservoir conditions. Consequently, most of the low water production rate over a well's life can be attributed to condensed water vapor.

Bossier Sand Intrinsic Rock Properties. We have also conducted a comprehensive description of the Bossier sands. These descriptions are based upon evaluations of more than 500 ft of whole core obtained from three wells in the Mimms Creek and Dew Fields. Our description includes classification of petrophysical rock types based on similar pore and grain scale characteristics, such as composition, texture, mineralogy, clay type, and types of diagenesis. We have also defined several hydraulic rock types representing similar ranges of storage and flow characteristics. Table 1 summarizes the various measurements made to describe the Bossier sands.

Petrographic Rock Types.¹⁴ The petrographic rock types observed within the Bossier Sands include; clean sandstone, argillaceous/weakly laminated sandstone, dolomitic sandstone, and argillaceous/burrowed siltstone. The Folk⁸ classification ranges from subarkose to sublitharenite to lithic wackes. The framework grains contain, on average, 84% quartz, 6.5% feldspar, and 9.5% rock fragments. The range for these constituents is 41%-94% for quartz, 0%-11.7% for feldspar, and 0.5%-59% for the rock fragments.

The intergranular constituents are comprised of prevalent quartz overgrowths, diagenetic clay in the sands, detrital clay found in sand and silt, dolomite cement, and local pyrite. The clay fraction is dominantly grain coating chlorite and illite. Texturally, the Bossier Sands have a narrow range of grain size, typically from upper very fine to fine (0.06-.30 mm). The sands are medium to well sorted, while the silts are typically poorly sorted. The grain shape is sub-angular to well rounded. A significant degree of compaction is observed in the form of suturing, elongation of grain contacts, and ductile grain deformation.

Bossier sands also exhibit a significant diagenetic overprint. Diagenesis, the physical or chemical processes that cause changes in the initial rock properties, tends to modify the initial pore structure and geometry. This results in an increase in the tortuosity from a reduction in pore throat size and a subsequent increase in the number of isolated and

disconnected pores. Most diagenetic effects are manifested as reductions in permeability and porosity. The most important forms of diagenesis in the Bossier sands are mechanical compaction, cementation from quartz overgrowths, grain-coating/pore lining clay development, and grain dissolution. Although less important and prevalent, carbonate cementation has also been observed in Bossier sandstones.

Hydraulic Rock Types.¹⁴ We have also identified several Bossier sand hydraulic rock types. When described on the basis of the dominant pore throat diameter determined from high-pressure mercury capillary pressure data, we observed distinct groupings of rocks with similar flow and storage properties, *i.e.*, hydraulic rock types. Figure 6 is an example of an incremental mercury intrusion plot used to identify rock types.⁹⁻¹⁴ Figure 7 shows the general region of each rock type in porosity-permeability space, while Table 2 lists the permeability, pore throat aperture size, and range of initial water saturation conditions. Rock types 1, 2A, 2B, and 3A are all considered as reservoir rock. Because of their low permeability, high initial water saturation and significant degree of vertical heterogeneity, rock types 3B and 4 are non-reservoir rocks and probably act as flow baffles, barriers, and seals.

Effective Porosity and Absolute Permeability. Figure 7 shows a typical distribution of Bossier sand porosity and permeability. Effective porosity varies from 1% to 17%, while absolute permeability ranges from 0.001 to 1 md. Non-reservoir and seal rocks have permeability values lower than 0.0001 md. In general, the Bonner and York sands have better permeability and porosity than the Moore and Shelley sands. Better reservoir quality combined with higher pressures is demonstrated by greater gas recovery.

Similar to most tight gas sands, the Bossier sands display both stress-dependent porosity and permeability characteristics. For example, the hyperbolic decline behavior exhibited by many tight gas sand wells can be attributed, in part, to reductions in permeability and porosity during the depletion history. We measured porosity and permeability over a wide range of stress conditions and observed slight changes in porosity. We did, however, measure significant reductions in permeability as net pressure increased. We also noticed the degree of stress dependency increased for the lower quality rock types.

Effective and Relative Permeability. Although we believe no mobile liquid phase exists in the Bossier sands at reservoir conditions, the presence of water does affect gas flow capacity. Consequently, we measured effective gas permeability for a range of water saturation. Figure 8 shows computed relative permeability curves for hydraulic rock types 1, 2A and 2B. All of the curves were normalized to 5% initial water saturation based on the minimum water saturation measured in rock type 1. Note that, for the entire range of hydraulic rock types, the effective permeability to gas is reduced significantly for water saturation greater than 40%.

Water Saturation. We also measured connate water saturation from more than 300 Bossier core plugs. Since the

whole core was obtained with a low invasion, oil-base mud system, we were able to obtain consistent and accurate estimates of in-situ connate water saturation. We used the Dean Stark solvent extraction technique with toluene as the solvent. Most of the non-reservoir rock had water saturation greatly exceeding 60%. Measured water saturation in the reservoir rock, however, ranged from 5% in hydraulic rock type 1 to 60% in hydraulic rock type 3A. These measured water saturations, especially in the best reservoir rock, were significantly lower than we expected. Consequently, we sought to verify these values with log-based calculations and capillary pressure characteristics.

Capillary Pressure Characteristics. We measured capillary pressure characteristics using high-pressure, mercury injection (MICP). We used MICP since the low porosity and permeability precluded using either centrifuge or porous plate methods that are limited by the maximum attainable pressure. From the capillary pressure measurements, we were able to describe the vertical water saturation distribution,¹⁵⁻¹⁷ range of irreducible water saturation, and capillary seal capacity. As discussed previously, we also identified hydraulic rock types using the capillary pressure characteristics.

To verify the water saturation measured from core plugs, we converted capillary pressures to height above free water and plotted them against water saturation. Geologic models of the Bossier sands in the Mimms Creek and Dew Fields indicate the sands were deposited on a low relief shelf/slope topography and appear to be laterally discontinuous, thus minimizing the total relief to about 200 ft. On the basis of a 200-ft total column height, the computed range of irreducible water saturation is 35% to 100% for the reservoir rocks. This range is significantly greater than the range measured from the core plugs. In addition, relative permeability measurements indicate very low gas productivity when water saturation is 40% or greater.

Reservoir Description Program to Quantify Water Saturation

To resolve the significant discrepancies between the core-based water saturation and those derived from capillary equilibrium calculations, we initiated a rigorous evaluation and validation program composed of three methods:

- Core-Based Measurements: direct water saturation measurements from Dean Stark extraction of core plugs;
- Log-Based Computations: computed vertical distribution of water saturation from well log response in three cored wells using measured Archie¹⁸ parameters;
- Capillary-Equilibrium-Based Computations: assuming capillary equilibrium, computed vertical distribution of water saturation using geological structure.

Core-Based Water Saturation Measurements. We obtained more than 500 ft of whole core from three wells in the Mimms Creek and Dew Fields. To minimize invasion effects and preserve connate water saturation, we used an oil-base mud system. Properties of the oil-base mud included

very low fluid loss as well as low surfactant energy. For most rock types, we consistently observed an invasion rind less than one inch in a four-inch diameter whole core, thus insuring accurate "preserved-state" water saturation measurements. Figure 9 illustrates a slightly larger invasion profile in one of the most permeable rocks (*i.e.*, hydraulic rock type 1). Note, however, we still observe an undisturbed portion of the core.

Water saturation was measured directly with the Dean Stark solvent extraction process using toluene as the solvent. On the basis of more than 300 plugs, we observed water saturations ranging from as low as 5% in the best reservoir rock to more than 60% in the poor quality or non-reservoir rock.

Log-Based Water Saturation Calculations. We also computed the vertical distribution of water saturation in the same wells from which the core was obtained. The best match between core-based and log-based water saturation was obtained with the Modified Simandoux shaly sand model.¹⁹ Shale volume was estimated from the gamma ray response and porosity cross-plot techniques. Effective porosity was computed using neutron-density cross-plot techniques and was corrected for shale and gas effects.

Application of the Modified Simandoux model¹⁹ also requires estimates of the Archie¹⁸ saturation exponent, n , and the cementation exponent, m . These parameters were measured in the laboratory using both two- and four-electrode resistivity devices. Core samples were saturated using a 220,000 ppm brine, and all measurements were made at initial reservoir conditions, *i.e.*, 3500 psia net stress and temperature of 300°F. Results from both two- and four-electrode devices were in close agreement. The average values of m and n were 2.15 and 1.85, respectively. We also measured excess conductance using the Co/Cw method. Average corrected values of m^* and n^* were 2.2 and 1.87, respectively. The effect is minimized by the highly saline connate water.

The final component required to compute connate water saturation is water resistivity, R_w , at reservoir conditions. Unfortunately, direct sampling and testing of the formation water is impractical in the Bossier sands in the Mimms Creek and Dew Fields. Low permeability and the associated relative permeability curves suggest a mobile water phase is improbable. Initial water produced from the Bossier is mostly fracturing fluids from the stimulation treatment. The water production following fracture clean-up is probably condensed water of vaporization with a very low salinity. Consequently, we used commutation analysis and fluid inclusion micro-thermometry to estimate connate water salinity.

Commutation or residual salt analysis is a process that extracts or leaches connate water and the associated salts from preserved core samples using ultra-pure, deionized water. Salt concentration and composition in the leachate are measured using an atomic absorption or mass spectrometer technique, while salinity is estimated from material balance calculations. Salinity measurements ranged from 220,000 ppm to 300,000 ppm.

Fluid inclusion micro-thermometry (FIT) uses thin sections from core samples to measure the temperature at which fluid inclusions melt. This melting temperature is directly related to the connate water salinity. Results from the FIT analysis ranged from 180,000 ppm to 240,000 ppm, which is consistent with results from the commutation analysis.

In general, results from the log-based analysis agreed with water saturation estimates from the core analysis in the reservoir rock. An example of this agreement is illustrated in Fig. 10. Some discrepancies were observed in the non-reservoir rock.

Capillary-Equilibrium-Based Water Saturation Calculations. As we discussed previously, we also attempted to compute a vertical distribution of water saturation from capillary pressure characteristics. We converted capillary pressures to height above free water and plotted them against water saturation. Our current understanding of the geology in the Bossier sands in the Mimms Creek and Dew Fields indicates the sands were deposited on a low relief shelf/slope topography and appear to be laterally discontinuous. Under these conditions, the total relief is about 200 ft. Using a 200-ft total column height, the computed range of irreducible water saturation is 35% to 100% for the reservoir rocks. This range, which is illustrated in Fig. 11 as the dashed horizontal line, is significantly greater than the core-based measurements and log-based calculations.

Because of these discrepancies, our next step was to determine the column height required to match the range of water saturations determined from core and log analyses. Our calculations indicate an average total column height of 1000 ft is required to generate irreducible water saturations from 5% to 55% for rock types 1 through 3A, respectively. As shown by a solid horizontal line in Fig. 11, this is consistent with the average seal capacity of the sealing facies. The capillary seal facies have a seal capacity ranging from 700 ft to 2000 ft and an average capacity of 1000 ft at a displacement saturation of 7.5%. This average seal capacity represents the upper threshold of column height for sands having 1000 ft of total relief. Current depositional and geological models of the Mimms Creek and Dew Fields do not, however, support a 1000 ft column height.

Sub Capillary-Equilibrium Water Saturation Concept. In summary, vertical distributions of core-derived measurements and log-derived calculations of water saturation cannot be matched with estimates from capillary pressure characteristics unless we make unrealistic assumptions about sand geology and structure, particularly column height. This observation suggests the vertical distribution of water saturation in the Bossier sands may not be in capillary equilibrium. In fact, measured water saturation is much lower than that which would be predicted by capillarity, *i.e.*, a sub capillary-equilibrium or sub-irreducible water saturation condition. Although not common in the petroleum industry, this phenomenon has been observed and documented in basin-centered gas systems.^{5,20-30}

Possible Mechanisms for Sub Capillary-Equilibrium Water Saturation Phenomenon

In this section, we present a hypothesis to explain the physical mechanisms and conditions that could cause the development of a sub capillary-equilibrium, water saturation distribution. We also present a geological process model under which this phenomenon would most likely occur. Our model is discussed as part of a total petroleum systems genesis but within the context of a basin centered gas accumulation. Attributes of basin centered gas systems are summarized in Table 3. Note that the Bossier sands and shales exhibit most of the properties listed in Table 3.

Elements of our Petroleum System Process Model are presented in Fig. 12. These elements – *i.e.*, source rock, reservoir rock, and reservoir seals - are very similar to conventional oil and gas systems. The reservoir rock is most often deposited as hydraulically isolated or disconnected sands interbedded with organic-rich marine shales. The sand-shale sequences usually occur as vertically stacked but isolated sands. As the sand-shale systems are buried by overlying deposits, the sands are buried deeper and exposed to higher pressures and temperatures. Continued burial and exposure to extreme environmental conditions causes the organic material to decay and generate hydrocarbons. Depending on not only the type and quantity of organic material but also the environmental conditions, the organic diagenesis occurs in several discrete stages, resulting in generation of both liquid and gas hydrocarbons. If the shales are exposed to high enough pressures and temperatures associated with the gas generation window, all hydrocarbons will be in the gas phase.

During all stages of shale diagenesis, hydrocarbons are frequently expelled from the shales and migrate into reservoir rock. If an adequate sealing system exists, then the hydrocarbons will be trapped in the reservoir rock. Sands in our model are isolated and interbedded with the shale, so shales most often act both as seals and local hydrocarbon sources. Continued hydrocarbon migration into the reservoir causes an increase in pore pressure until the shale seal capacity is exceeded, causing hydrocarbons to be expelled. Hydrocarbon expulsion continues until the reservoir pore pressure equilibrates with the shale seal capacity. At this point the shale heals and re-seals. As long as hydrocarbons are generated, the process becomes cyclical. We have given the cyclical process the acronym GENPERR (hydrocarbon generation, pressurizing, expelling, re-sealing, and recharging). This cyclical process to explain the petroleum system genesis has been documented by others.^{5,20-23,29,30}

The critical element in our model is a mechanism to effectively remove connate water and transport the water up the vertical section. It has been recognized that several mechanisms can remove connate water from reservoir rock.³⁰ None of these mechanisms alone, however, has the potential for removing large connate water volumes and establishing a sub capillary-equilibrium, water saturation distribution. Most shales, even those with natural fractures, have a very low

effective permeability to water. In addition, liquid water displacement by hydrocarbon gas is not a very effective mechanism for removing the water.

Consequently, we have identified another mechanism for removing the connate water. We believe the key element required to remove water effectively is the process of vaporizing connate water into the gas phase. Laboratory data suggests that, at pressures exceeding 10,000 psia and temperatures exceeding 350°F, significant volumes of water vapor may be dissolved in the hydrocarbon gas.³¹ Furthermore, the solubility of water vapor in gas is enhanced when non-hydrocarbon gases, such as CO₂ and H₂S, are present. We believe that most of the connate water displaced from reservoir rock is in the form of water vapor dissolved in the hydrocarbon gas. Gas generated and expelled from the shales is dry (*i.e.*, initially no dissolved water vapor). As long as hydrocarbon gases continue to migrate into the reservoir, we have a mechanism to continuously vaporize and effectively remove connate water.

The final element required to explain a sub capillary-equilibrium water saturation distribution is related to the hydrocarbon generation potential of the shales. For very organic-rich shales, hydrocarbon generation and migration may continue for millions of years. Furthermore, if hydrocarbon migration into the reservoir is still ongoing and if the migration rate exceeds the rate at which hydrocarbons are expelled, then the reservoir conditions will be dynamic (albeit at very slow rates) rather than static. Under normal conditions, a vertical distribution of water saturation in capillary equilibrium (*i.e.*, static conditions) suggests surface wetting or adhesion forces are exactly balanced by gravitational forces. If, however, we have an external source of energy (*i.e.*, influx of gas from source rock), then the vertical water saturation distribution cannot be in capillary equilibrium and we would not expect to encounter static conditions.

Summary and Conclusions

We have documented an apparent sub capillary-equilibrium water saturation distribution in the Bossier sands in the Mimms Creek and Dew Fields, Freestone Co., TX. Our observations are based on consistent measurements from several different techniques and data sources. We have also postulated that the Mimms Creek and Dew Fields may be part of a basin centered gas system, and the mechanisms responsible for that system may have contributed to the unusually low water saturation. We also believe that the Bossier sands in the Mimms Creek and Dew Fields are not in capillary equilibrium. Finally, we have identified and provided evidence that water vaporization and dissolution in the hydrocarbon gas may be an effective mechanism for removing and transporting connate water up the vertical column.³³

Acknowledgments

We would like to express our thanks to Anadarko Petroleum Corp. and Hycal Energy Research Laboratories, Ltd. for permission to publish this paper. Special thanks to Kevin Hae Hae for his editorial input on the Bossier sand geology.

References

- Prouty, J.L.: "Tight Gas in the Spotlight," in *GasTIPS*, Gavin, J.J. and Lang, K.R. (Editors), Gas Technology Institute, vol. 7, no. 2, Chicago, IL (2001), pp. 4-10.
- Montgomery, S.: "East Texas Basin Bossier Gas Play in *Petroleum Frontiers*, Anderson, J., ed., IHS Energy Group, Englewood CO (2000), pp 1-60.
- Perrizela, P., 2002, "OMNI Core description reports, McAdams A7, Henderson 6, and Burgher D7.
- Espitalie, J., Deroo, G., and Marquis, F., 1985, "La pyrolyse Rock-Eval et ses applications", *Rev. Inst. Fr. Pet.* 40, pp 563-579, pp 755-784, *Rev. Inst. Fr. Pet.* 41, pp 73-89.
- Hunt, J.M., 1990, "Generation and migration of petroleum from abnormally pressured fluid compartments", *AAPG Bulletin*, vol. 74, no.1 (January 1990), p.1-12.
- Swarbrick, R.E., and Osborne, M.J., 1998, "Mechanisms That Generate Abnormal Pressures: An Overview", in Law, B.E., G.F. Uimishek, and V.I. Slavin, eds. *Abnormal pressures in hydrocarbon environments: AAPG Memoir 70*, p. 13-34.
- Finkbeiner, T., Zoback, M., Flemmings, P., and Stump, B., "Stress, pore pressure, and dynamically constrained hydrocarbon columns in the South Eugene Island 330, northern Gulf of Mexico", *AAPG Bulletin*, v.85, no.6 (June 2001), p. 1007-1031.
- Folk, R.L., 1974, "Petrology of Sedimentary Rocks", Hemphill Publishing Co., Austin, Tx, 78703.
- Pittman, E.D., 1992, "Relationship of Porosity and Permeability to Various Parameters Derived From Mercury Injection-Capillary Pressure Curves for Sandstone", *AAPG*, v. 76, No. 2 (Feb. 1992) 191-198.
- Gunter, G.W., et al. "Early Determination of Reservoir Flow Units Using an Integrated Petrophysical Model," paper SPE 38679 presented at the 1997 SPE Annual Technical Conference and Exhibition, San Antonio, TX, October 5-8.
- Washburn, E.W., 1921, "Note On A Method of Determining the Distribution of Pore Sizes In A Porous Material", *Proceedings of the National Academy of Science*, V. 7, p.115-116.
- Swanson, B.F., 1979 "A Simple Correlation Between Permeabilities and Mercury Capillary Pressure", paper SPE 8234, 54th Annual Technical Conference and Exhibition, Las Vegas, NV, Sept. 23-26, 1979.
- Thompson, A.H., et al.: "Estimation of Absolute Permeability From Capillary Pressure Measurements", paper SPE 16794 presented at the 1987 SPE Annual Technical Conference and Exhibition, Dallas, Tx., Sept. 27-30.
- Newsham, K.E., Rushing J., An Integrated Work-Flow Model to Characterize Unconventional Gas Resources—Part I: Geological Assessment and Petrophysical Evaluation," paper SPE 71351 presented at the 2001 SPE Annual Technical Conference and Exhibition, New Orleans, LA, Oct. 1-3.
- Leverett, M.C., 1941, "Capillary Behavior in Porous Sands", *Trans. AIME*, 1941.
- Gunter, G. et al., 1999, "Saturation Modeling At the Well Log Scale Using Petrophysical Rock Types and a Classic Non-Resistivity Based Method", 40th Annual SPWL Symposium, Paper ZZ
- Negabahn, S. et al., 2000, "An Improved Empirical Approach For Prediction of Formation Water Saturation and Free Water Level For Uni-Modal Pore Systems", SPE 63282, 2000 SPE Annual Technical Conference and Exhibit, Dallas, Tx., October 1-4, 2000.
- Archie, G.E., 1950, "Introduction to Petrophysics of Reservoir Rocks", *AAPG Bulletin*, V.34, p.943-961.
- Simandoux, P., 1963, "Mesures dielectrique en milieux poreux, application a mesure de saturation en eau, etude des massifs argileux", *Revue de l'institut Francais du Petrole*, Supplement issue, 1963, p. 193-215.
- Law, B. E., 1984a, Relationships of source rocks, thermal maturity, and overpressuring to gas generation and occurrence in low-permeability Upper Cretaceous and lower Tertiary rocks, Greater Green River Basin, Wyoming, Colorado, and Utah, in Woodward, J., Meissner, F.F., and Clayton, J.L., eds., *Hydrocarbon source rocks of the greater Rocky Mountain region: Rocky Mountain Association of Geologists*, p. 469-490.
- Law, B.E., 1984b, ed., Geological characteristics of low-permeability Upper Cretaceous and lower Tertiary rocks in the Pinedale anticline area, Sublette County, Wyoming: U.S. Geological Survey Open-File Report 84-753, 107 p
- Law, B.E., and Dickinson, W.W., 1985, A conceptual model for the origin of abnormally pressured gas accumulations in low-permeability reservoirs: *AAPG Bull.*, v.69, p.1295-1304.
- Law, B.E., 1995, Columbia Basin-Basin-centered gas play (0503), in Tennyson, M.E., Eastern Oregon Washington Province (005), in Gautier, D.L., Dolton, G.L., Takahashi, K.I., and Varnes, K., eds., 1995 National Assessment in the United States of oil and gas resources: results, methodology, and supporting data: U.S. Geological Survey Data Series 30.
- Masters, J.A., 1979, Deep basin gas trap, western Canada: *AAPG Bull.*, v. 63, p.152-181.
- Masters, J.A., 1984, ed., Elmworth - Case study of a deep basin gas field: *AAPG Memoir 38*, 316 p.
- Ryder, R.T., SanFilipo, J.R., Hettinger, R.D., Keighin, C.W., Law, B.E., Nuccio, V.F., Perry, W.J., and Wandrey, C.J., 1996, Continuous-type (basin-centered) gas accumulation in the Lower Silurian "Clinton" sands, Medina Group, and Tuscarora Sandstone in the Appalachian Basin: *AAPG Bull.*, v. 80, p. 1531.
- Nuccio, V.F., Schmoker, J.W., and Fouch, T.D., 1992, Thermal maturity, porosity, and lithofacies relationships applied to gas generation and production in Cretaceous and Tertiary low-permeability (tight) sandstones, Uinta Basin, Utah., in Fouch, T.D., Nuccio, V.F., Chidsey, T.C., Jr., eds., *Hydrocarbon and mineral resources of the Uinta Basin, Utah and Colorado: Utah Geological Association Guidebook 20*, p. 77-94.
- Matinsen, R.S, 1994, "Summary of published literature on anomalous pressures: implications for the study of pressure compartments", in Ortoleva, P.J. ed., *AAPG Mem 61*, 1994.
- Spencer, C.W., 1987, "Hydrocarbon generation as a mechanism for overpressuring in the Rocky Mountain region", *AAPG Bulletin* vol. 71, no. 4 (April 1987), p.368-388.
- Meissner, F.F, 1987, "Mechanisms and patterns of gas generation/storage/expulsion-migration/accumulation associated with coals measures in the Green River and San Juan Basins, Rocky Mtn. Region, USA, in Dolgigez, B., ed., "Migration of hydrocarbons in sedimentary basins, 2nd IFP Exploration Research Conf., Carcias, France, June 15-19, 1987, Editions Technip. Paris, p. 79-112
- McCain, W.D., 1990, "The properties of petroleum fluids", 2nd Ed., Penwell Publishing Co. 548p.

Table 1. Typical Core Analysis Methods For Bossier Sand Description

Measurement Method	Primary Objective of Measurement
1) Routine helium porosity, unsteady-state permeability (horizontal P&P)	1) Provide a reservoir storage and flow capacity profile, rock type identification
2) Dean Stark fluid extraction from oil-based core	2) Describe the initial water saturation (Sw) conditions and profile; determine irreducible Sw
3) Slab core, polish slab face, and photo core using reflected white light and ultra violet light source	3) Describe sedimentary structures for genetic units, sequence, and depositional environment, observe mud invasion front as an early indicator of permeability.
4) Stressed dependent P&P	4) Describe the in-situ P&P, and Sw properties and observe the loss of P&P through a simulated depletion history.
5) X,Y,Z oriented P&P	5) Fully describe the permeability tensor and associated anisotropy.
6) Thin section photo micrographs, epifluoresence	6) Point counts for composition, grain size, sorting, pore distribution, paragenetic description, and petrographic rock typing
7) Stressed thin section photo micrographs, epifluoresence	7) Describe occurrence of in-situ micro-cracks
8) Xray diffraction (XRD), Fourier transform infrared spectroscopy (FTIR)	8) Relative abundance mineral presence and abundance.
9) Scanning electron microscopic surveys (SEM)	9) Describe pore geometry, clay type and habitat, micro-crack morphology
10) High pressure mercury, capillary injection (MICP)	10) Describe pore throat aperture, porosity, permeability, hydraulic rock type, irreducible Sw, seal capacity, and interpreted for hydrocarbon column height, and Sw profiles.
11) Electrical properties; Fr vs. porosity, Ri vs Sw, Co/Cw	11) Describe the the Archie parameters used for estimating Sw, correct "m" and "n" for excess conductance to "m*" and "n*".
12) Compression tests; unconfined compressive strength, hydrostatic, triaxial, Brazilian, uniaxial-depletion stress path	12) Describe the elastic moduli (Young's and Poisson's Ratio), strength envelope of each rock type, grain, bulk, and pore volume compressibility and the critical drawdown pressure at which rock failure occurs.
13) Regained permeability	13) Describe the rock-fluid interaction of various fluid types and the associated loss of permeability
14) Incremental phase trap, relative permeability	14) Describe the permeability of gas to flow under partial saturation conditions for each hydraulic rock type. Used in combination with the stressed dependent absolute permeability to describe effective permeability.
15) Commutation and fluid inclusion micro-thermometry	15) Determine the formation water salinity

Table 2. Bossier Sand Hydraulic Rock Type Physical Range of Attributes.

Hydraulic Rock Type	Absolute Permeability, mD @ 800 psi	Pore Throat Radius, μ	Initial Water Saturation @ 1000' HAFW, %
1	$k_a > 0.5$	> 0.6	5 - 15
2A	$0.5 > k_a > 0.05$	$0.6 > r > 0.18$	10 - 30
2B	$0.05 > k_a > 0.015$	$0.18 > r > 0.10$	25 - 40
3A	$0.015 > k_a > 0.003$	$0.10 > r > 0.05$	35 - 45
3B	$0.003 > k_a > 0.00013$	$0.05 > r > 0.01$	40 - 55
4	$K_a < 0.00013$	$r > 0.01$	> 55

Table 3. Common Attributes of Basin Centered Gas Systems

Attribute Description
1) Geologic properties
Cretaceous Age ^{24,25}
Reservoirs may be single, isolated sand bodies or vertically stacked sands several 1000 feet thick ²⁰⁻²³
Structure and stratigraphy play a secondary role in the hydrocarbon accumulation ^{20-25, 27}
Top of BCGS as defined by top of abnormal pressure (TAG) cut across both structure and stratigraphy ^{24,25}
2) Shale characteristics and hydrocarbon generation potential
Local interbedded source rock ²⁷
Vitrinite > 1.1 ²⁶
Top of BCGS $> 0.7\%$ Ro ²⁰⁻²³
Gas migration distance is short ²⁰⁻²³
Gas of thermal origin ²⁰⁻²⁵
Regionally pervasive gas accumulations, gas prone source rock ²⁰⁻²⁵
3) Abnormal pressure and temperature gradients
Primary pressure mechanism is hydrocarbon generation ²⁰⁻²³
Abnormally pressured gas accumulations (under and over pressure) ^{20-25, 26}
Formation temperatures $> 150F$ ²⁶
4) Rock and fluid properties
High formation water salinity; 200k - 300k TDS ²⁶
Low permeability, typically < 1 mD ²⁰⁻²⁶
Water most often present as irreducible (non-mobile) water ^{20-23, 26}
Variable temporal seal integrity ²⁰⁻²³
Porosity less than 13% ^{20-23, 26}
5) Production properties
Average water yield (beyond load water) 1 - 20 BW / MMSCF gas ²⁶
Fracture stimulation required for commercial production ^{24,25}
Gas accumulations are down dip from normally pressured, water bearing reservoirs ^{24,25,27}
Gas accumulations do not have down dip water contacts ²⁰⁻²⁵
Large in-place hydrocarbon volume ²⁷
Low recovery factors ²⁷

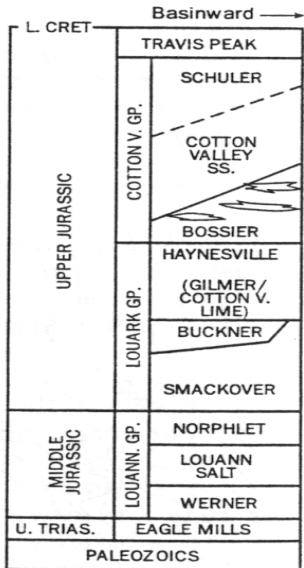


Figure 1. East Texas Stratigraphic Section. The Bossier Sands are of Jurassic age found in the Lower Cotton Valley Group. From Montgomery (2000) ².

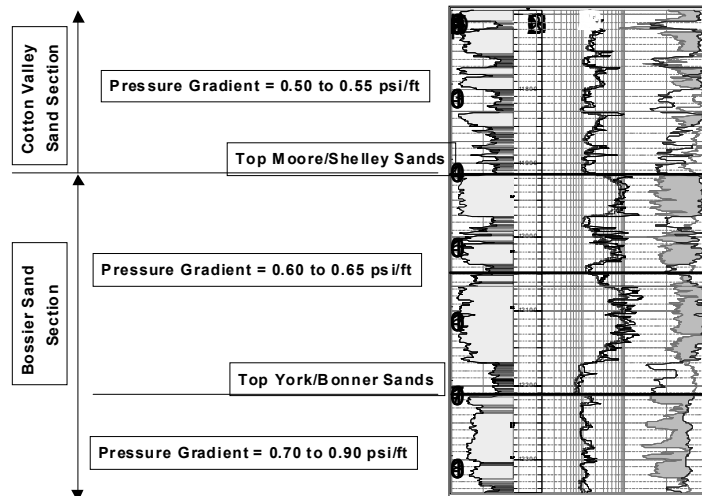


Figure 3. Type log of the Bossier Sands showing the range of observed pressure gradients and the sequence of sand deposition.

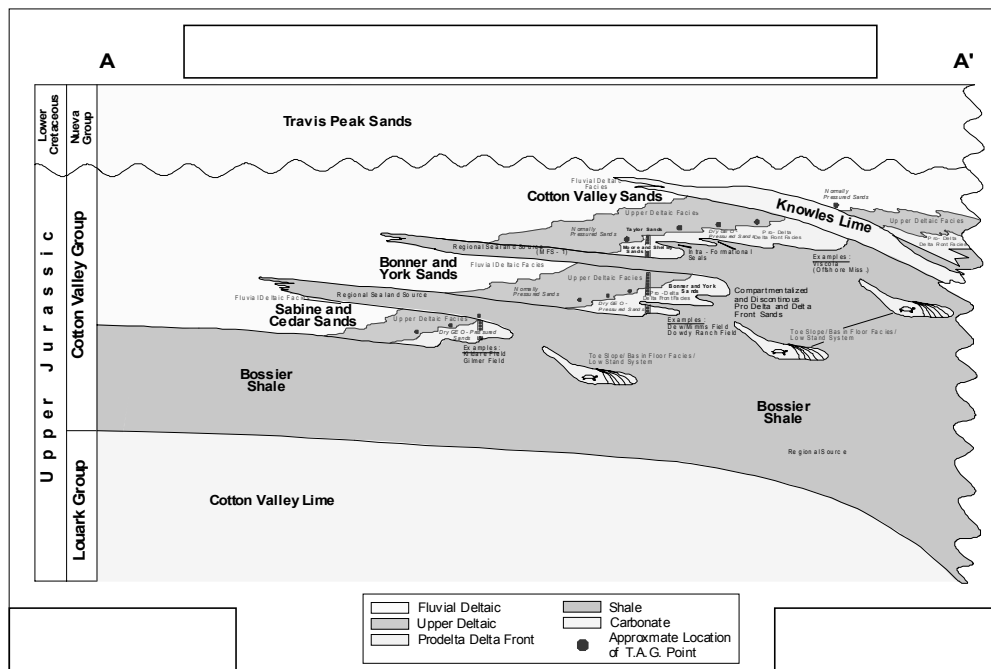


Figure 2. Generalized regional dip-section of the Bossier facies. Sand deposition represents cycles of sand progradation into the basin onto organic rich mud, succeeded by marine transgression. Much of the Bossier shales down dip appear to be time equivalent to the up dip Cotton Valley Sandstone and represent pro-delta/delta front material related to Cotton Valley deltaic systems (drawing courtesy of Jim Tautfest, Anadarko Petroleum Corp., 1999).

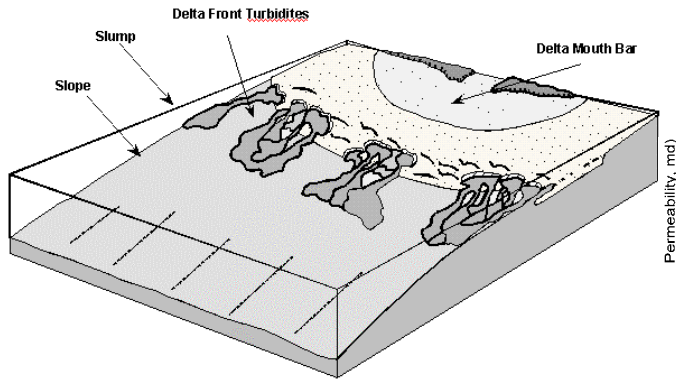


Figure 4. Typical Bossier sand body geometry is elongated and oriented with the long axis parallel to the depositional dip. Lateral sand continuity along depositional strike is often limited, resulting in sands with small dimensions and limited continuity. The sand body thickness varies from tens to several hundred feet.

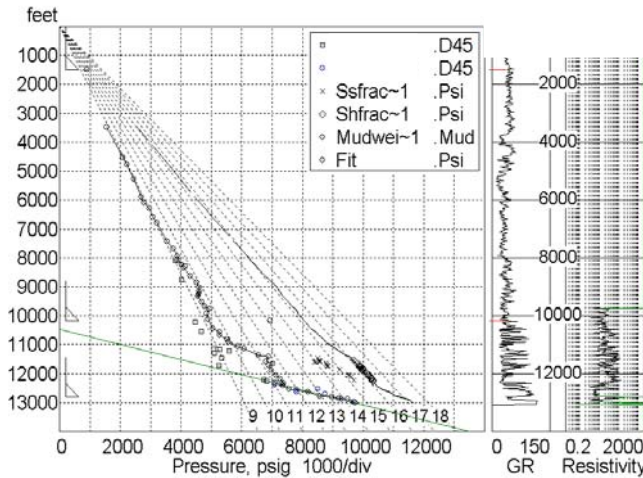


Figure 5. An example of a typical vertical pressure distribution estimated from the acoustic log response.

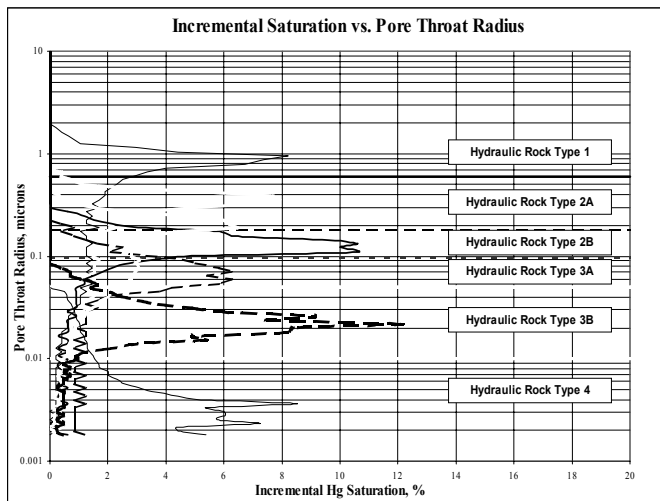


Figure 6. Incremental mercury intrusion plot used to identify rock types for the Bossier Sands.

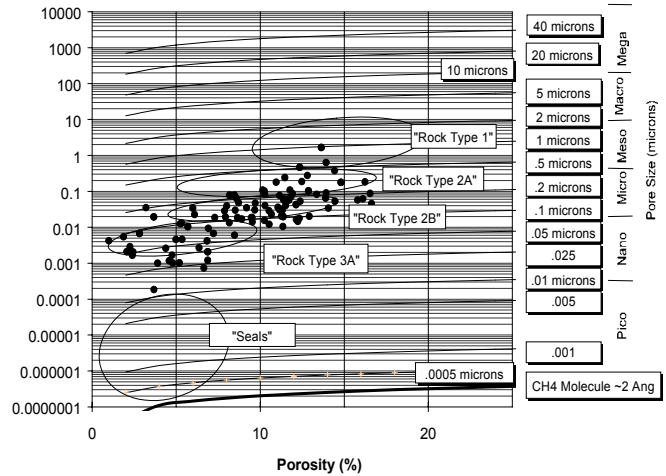


Figure 7. Porosity and permeability plot that shows the general region of each rock type (ovals) for the Bossier Sand.

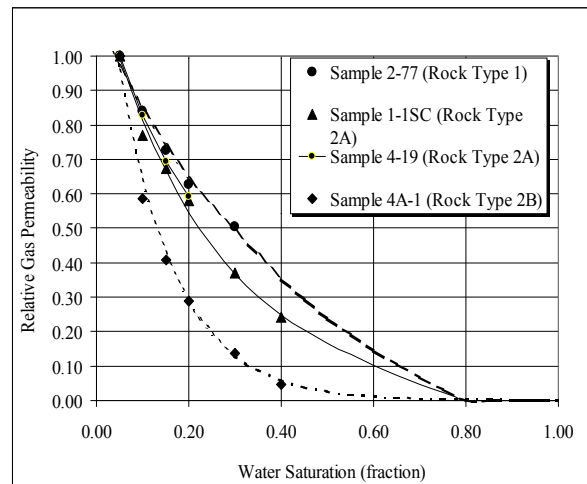


Figure 8. Relative permeability curves for hydraulic rock types 1, 2A and 2B. All of the curves were normalized to 5% initial water saturation based on the minimum water saturation measured in rock type 1.

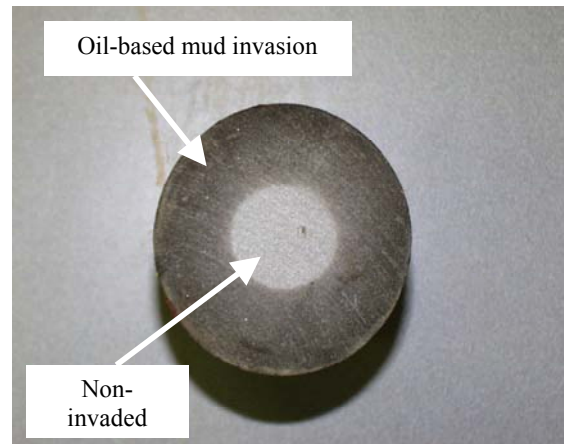


Figure 9. Photograph of a whole core section that illustrates the oil-based mud invasion profile in one of the most permeable rocks (*i.e.*, hydraulic rock type 1). Note, however, we still observe an undisturbed portion of the core.

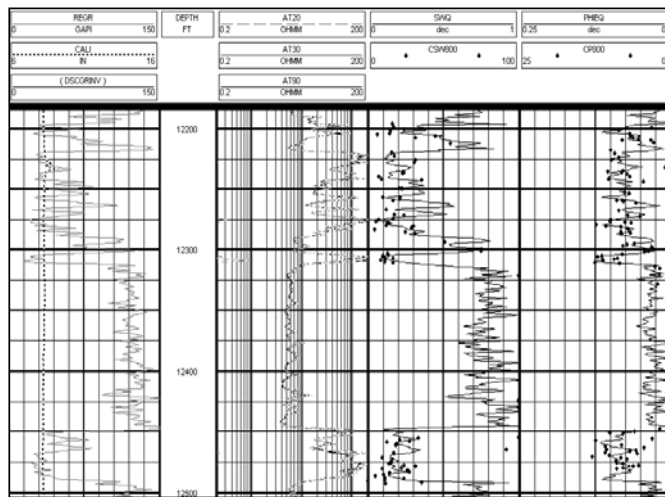


Figure 10. Log profile of gamma ray (track 1), resistivity (track 2), water saturation (track 3), and porosity (track 4). The measured water saturation and porosity from the core are represented by the discrete dots. Note that there is close agreement between the core and log values for both water saturation and porosity.

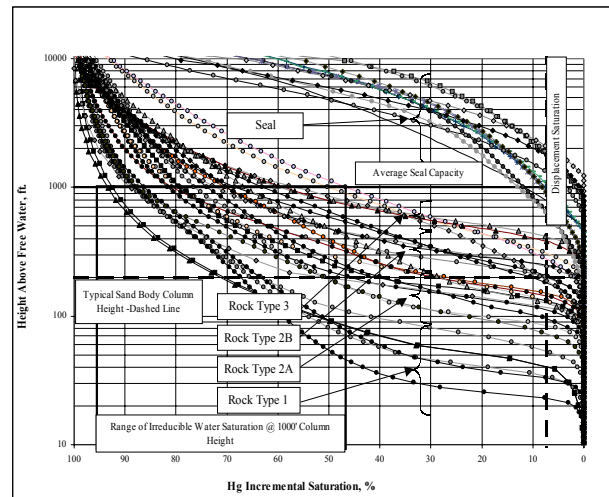


Figure 11. High pressure, mercury injection capillary pressure data converted to height above free water level. Note that the range of initial water saturation at 200' of column height is 30%-100%. It takes 1000'-2000' of column height to have water saturation in the measured range of 5%-40%.

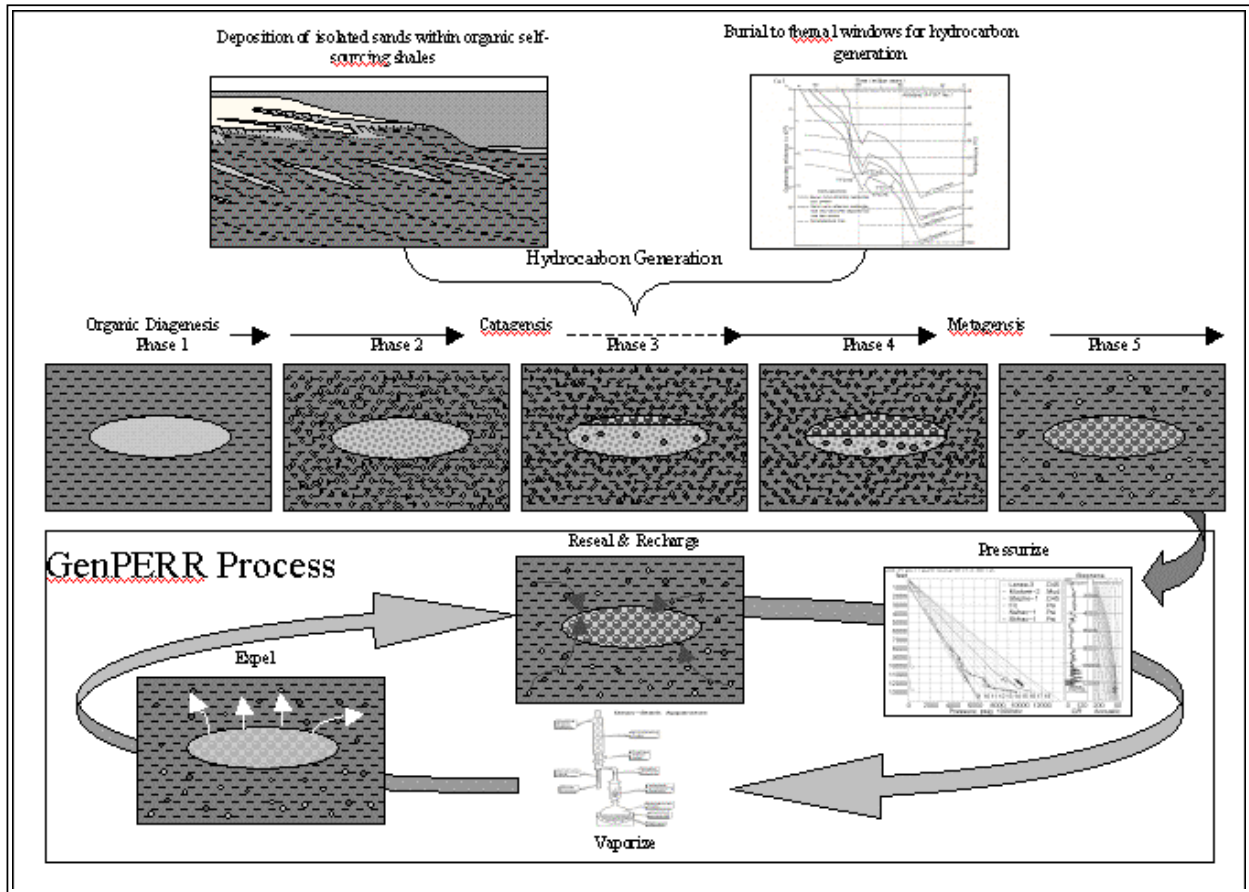


Figure 12. Elements of our Petroleum System Process Model: 1) Deposition of hydraulically isolated and low relief sands bodies onto organic rich, self-sourcing shale facies 2) Burial of sand and increase in temperature and pressure 3) Hydrocarbon generation via organic diagenesis 4) Local hydrocarbon migration into isolated sand bodies 5) In-situ hydrocarbon catagenesis, and metagenesis causing a build up of pressure from the fluid volume exchange and the removal of all but the irreducible pore waters 6) Cyclic process of: a) pressurizing the isolated sand bodies b) vaporizing the irreducible pore fluids c) leaking due to seal breach by the abnormal pressure d) resealing of the seal facies once the pressure has decreased below the seal pressure e) recharging by interbedded organic shales that continue today to generate hydrocarbons at a greater rate than they can be diffused (the pump is still on).